Pure metallic iron and hercynite in Eucrite imply a thermal condition after impaction. Zhuang Guo[1,2], Yang Li[1], Hongyi Chen[3], Shiejie Li[1], Xiongyao Li[1], Shen Liu[2], Shijie Wang[1]. [1]Institute of Geochemistry, Chinese Academy of Sciences, Guiyang, China; [2]Northwest university, Xi'an, China; [3]Guilin University of technology, Guilin, China.
E-mail: liyang@mail.gyig.ac.cn

Introduction: The Howardites-Eucrite-Diogenite (HED) clan of meteorites are generally considered to be derived from the Vesta asteroid [1-2]. Previous study demonstrated the pressure of the impact event on vesta is below 15GPa, as well as few high-pressure minerals have been found in HED meteorites [3-4]. Thermal metamorphic event is a significant stage of Vesta evolution, and the temperature is ranging from ~700 to 1000 ℃ [5]. Iron metal veins (most with minor Ni) had been reported in HED meteorites, which is attributed to the fluid deposition during the fluid-driven secondary alteration stage on Vesta [6]. Spinel is a common minor mineral in HED meteorites, dominantly of Cr-spinel [7].

Our work focuses on the observation of pure metallic iron and hercynite particles in the shocked melt pocket of Northwest Africa 11592 (NWA 11592). According to the results of HR-TEM observation and quantitative EDS mapping, the pure metallic iron and hercynite were determined in the meteorite, indicating a thermal condition of Vesta.

Sample and analytical techniques: NWA 11592 was found in Algeria, 2016, and was classified as basaltic Eucrite. The polished thin section of NWA 11592 was observed and analyzed by the FEI Scios dual-beam scanning microscope. The mineral composition was analyzed by JEOL 8230 electron microprobe (EPMA). Two FIB cross sections were prepared by the FEI Scios focus ion beam and analyzed by FEI Talos field-emission scanning transmission electron microscope.

Results: Petrology of host rock and shocked melt pocket. NWA 11592 is a basaltic Eucrite that mainly consists of pyroxene and plagioclase with an ophitic texture, as well as minor amounts of olivine, troilite, chromite and ilmenite. Augite exsolution lamella was universally observed within the pyroxene. The average compositions of host pyroxene ($Fs_{57.8\text{-}63.1}Wo_{2.05\text{-}6.75}$) and augite ($Fs_{26.6\text{-}27.4}Wo_{44.4\text{-}45.3}$) suggest an average equilibrium temperature about 850℃ [8].

Most Plagioclase crystals ($An_{88.1}Or_{0.7}$) exhibit atypical crystallization characteristics (not completely transformed into maskelynite), and its Raman spectrum shows diffuse broad peaks. All these mineral grains exhibit numerous thin cracks, which are attribute to the impact events on Vesta.

There are two thin shock-induced melt veins (~100μm wide) and one shocked melt pocket (~300μm wide) are observed in NWA 11592 (Fig 1a.). Both of veins exhibit amorphous glass with the composition of mixture of pyroxene and Plagioclase in host rock. Our work focused on the melt pocket with typical quench texture characterized by the dark needle-like material within the fine-grained matrix, as well as abundant metallic iron particles (~200nm) attach to the needle-like material (Fig 1c.).

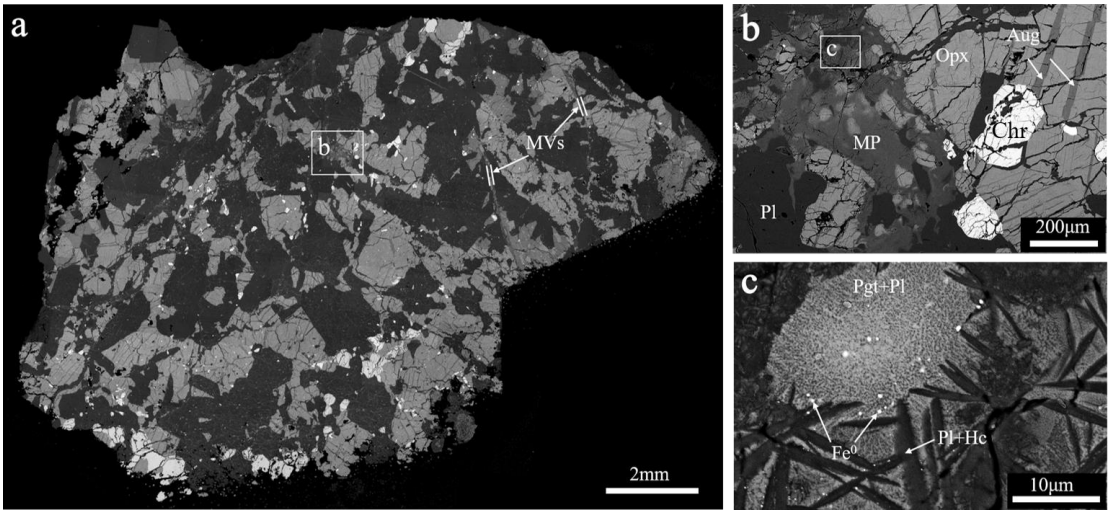

Fig 1. (a) BSE mapping of the Northwest Africa 11592. MVs: melt veins. (b)The BSE image of shocked melt pocket in NWA 11592. MP: melt pocket; Pl: plagioclase; Opx: orthopyroxene; Aug: Augite; Chr: chromite. (c) The high magnification BSE image of quench texture in melt pocket. Pgt+Pl: pigeonite and plagioclase; Pl+Hc: plagioclase and hercynite.

Two FIB cross sections were prepared in our study. The result of EDS mapping of TEM showing pure metallic iron particles without Ni and S content, as well as the FFT pattern can be index with the α-Fe (Fig 2.). The matrix of the shocked pocket mainly composed of sub-micron scale plagioclase and pigeonite crystals.

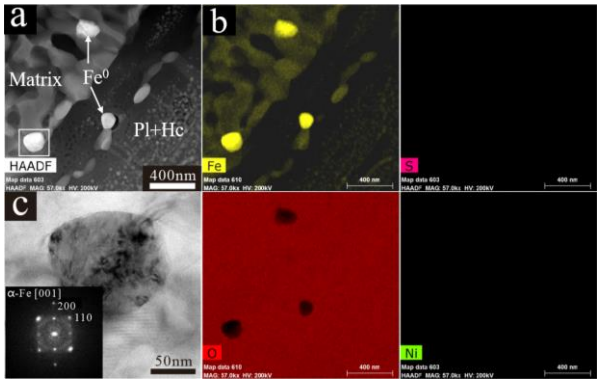

Fig 2. (a)HAADF image of part of the FIB cross section, and white square represents the location of Fig 2c. Pl+Hc: plagioclase and hercynite. (b) The result of the EDS mapping of Fig 2a. by TEM. (c) HR-TEM image of metallic iron particle. The inserted image is the FFT pattern of the HR-TEM image.

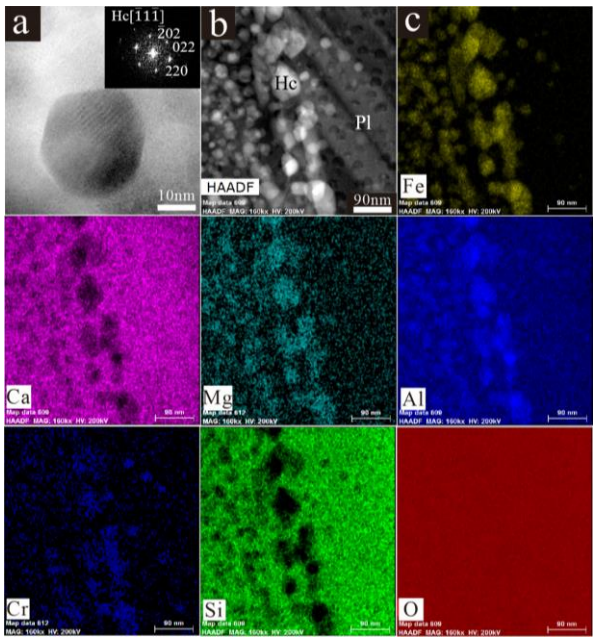

Fig 3. (a) HR-TEM image of hercynite grain. The inserted image is the FFT pattern of the HR-TEM image. (b)HAADF image of part of the FIB cross section. Hc: hercynite; Pl: plagioclase. (c) The result of the EDS mapping of Fig 3b. by TEM.

Besides, abundant Nano-sized hercynite crystals (~20nm) embedded in the plagioclase that does not crystallize well were confirmed by the TEM analysis. According to the quantitative EDS data of TEM, the hercynite with the composition of $(Mg_{0.20}Fe_{0.74})(Al_{0.97}Cr_{0.04})_2O_4$, and FFT patterns of HRTEM images of those grains show the cubic structure, which can be indexed with the hercynite (Fig 3.).

Discussion: Sub-micron scale metallic iron particles and matrix, needle-like plagioclase, as well as the Nano-sized hercynite grains imply these mineral assemblages crystallized in a very short time. The absence of flow feature and the oxidation of those pure iron particles rule out exotic origin [9]. Although the decomposition of mafic silicate mineral is known as the main reason for the formation of Fe^0 in meteorite [10], very small amounts of silica were found in this sample, so the source of Fe is questionable. The presence of the hercynite grains indicate the formation temperature is above 1310℃ [11]. To achieve temperature at zero pressure exceeding 1310℃, unrealistically high shock pressure(> 80GPa) is needed [12]. One possible scenario is that the shock occurred during the thermal metamorphism, which can provide high enough temperature to form these mineral assemblages, in this case, ~30GPa of peak pressure was required to form hercynite. In this meteorite, we did not observe any high-pressure minerals, which may be attributed to the longstanding temperature of thermal metamorphism on Vesta is not conducive to the preservation of high-pressure minerals [13].

References: [1] Mccord T B, Adams J B, Johnson T V. (1970) Science, 168(3938): 1445-1447. [2] Greenwood R C, Barrat J A, Yamaguchi A, et al. (2014) EPSL, 390(4): 165-174. [3] Stöffler D, Keil K, Scott E R D. (1991) GCA, 55(12): 3845-3867. [4] Pang R L, Zhang A C, Wang S Z, et al. (2016) Scientific Reports, 6(1):26063. [5] Schwartz and Mccallum J. (2005) American Mineralogist, 90(11-12): 1871-1886. [6] Warren, P.H., Rubin, A.E., Isa, J., Gessler, N., Ahn, I., Choi, B.-G. (2014) GCA, 141:199-227. [7] Mittlefehldt D W. (2015) Chemie der Erde-Geochemistry, 75(2): 155-183. [8] Kumar, Naresh, et al. (2014) Environmental Science & Technology, 48(23): 13888-13894. [9] Taylor W R. (1998) N.jb.miner.abh,172(2):381-408. [10] Moortèle B. Van de., B. Reynard, et al. (2007) EPSL, 262, 37-49. [11] Chen J, Yu L, Sun J, et al. (2011) Journal of the European Ceramic Society, 31(3):259-263. [12] Benzerara Karim., Francois Guyot, et al. (2002) American Mineralogist, 87, 1250-1256. [13] Ioannis B, Asimow P D, Jinping H, et al. (2018) Scientific reports, 8(1):9851-.